Journal of Bridge Engineering. Submitted October 25, 2010; accepted May 24, 2011;
posted ahead of print May 26, 2011. doi:10.1061/(ASCE)BE.1943-5592.0000274

Advanced numerical modeling of cracked tubular K joints: BEM and FEM comparison

L. Borges [a *], S.P. Chiew [b], A. Nussbaumer [c], C.K. Lee [b]

[a] BG Consulting Engineers, Avenue de Cour 61, CP 241, 1001, Lausanne, Switzerland
[b] School of Civil and Environmental Engineering, Nanyang Technological University, 50, Nanyang Avenue, Singapore 639798
[c] EPFL, Swiss Federal Institute of Technology of Lausanne, ICOM - Steel Structures Laboratory, School of Architecture, Civil and Environmental Engineering, 1015 Lausanne, Switzerland

ABSTRACT

A critical aspect in the design of tubular bridges is the fatigue performance of the structural joints. The estimation of a fatigue crack life using the Linear Elastic Fracture Mechanics (LEFM) theory involves the calculation of stress intensity factors (SIF) at a number of discrete crack depths. The most direct way is to carry out modeling by either the finite element method (FEM) or the boundary element method (BEM). For tubular joints commonly found in tubular bridges and off-shore structures, due to the complicated geometry resulted from the tubes intersection and welding, the construction of the numerical model often becomes a complex process. This paper presents two different model construction techniques that have been developed independently at the Swiss Federal Institute of Technology (EPFL) and the Nanyang Technological University (NTU), Singapore that are based in the BEM and the FEM, respectively. The SIF values obtained by these two methods are compared. It is found that so long as consistent geometrical models are employed, compatible SIF values could be obtained by both approaches. The best and the most consistent values are obtained for the deepest point along the crack front and are to be used for fatigue life computations.

Keywords: Boundary elements, Finite elements, Fracture mechanics, Stress intensity factors, Welded joints, Tubular bridges, K-joints

* Corresponding author: Tel: +41 21 6181117 32, Fax: +41 21 6181122
Email: luis.borges@bg-21.com (Luis Borges)

Accepted Manuscript
Not Copyedited

Copyright 2011 by the American Society of Civil Engineers

Journal of Bridge Engineering. Submitted October 25, 2010; accepted May 24, 2011;
posted ahead of print May 26, 2011. doi:10.1061/(ASCE)BE.1943-5592.0000274

INTRODUCTION

The need for aesthetics and architectural transparency has impelled engineers and architects to search for innovative solutions. A rational use of hollow sections leads to cleaner and more spacious structures. This is also true for bridge designs (Eekhout 1991). The relatively new concept of steel-concrete composite Circular Hollow Section (CHS) truss bridges presents the designer with new challenges, in particular with respect to the fatigue design of the CHS joints. Recent design and construction of many welded tubular truss bridges in Europe (Figure 1) have highlighted specific concerns about the behavior of the CHS joints subjected to cycle loading. The CHS K-joint configuration has been widely encountered and many researchers are interested to study the fatigue and crack growth behavior of these joints to predict the service life. The prediction of fatigue life of cracked CHS K-joints depends very much on the accuracy of its stress intensity factors (SIFs). Although many researchers have carried out extensive work on SIFs, reliable and accurate formulas of SIFs for cracked K-joints are seldom found in literature. This is largely due to the difficulty in creating complicated model of the weld profile and the doubly curved crack surface for accurate estimations of the SIF value. Lee and Bowness (2002) proposed an indirect method to estimate the SIFs for CHS K-joints based on plate-to-plate welded T-joints. However, their results are found to be very conservative.

Several published studies have been focusing on simplified methods that allow for fatigue life estimation. The most popular approached is the Hot Spot Stress (HSS) method (CIDECT 2001, AASHTO 2010, AWS 2008). In many cases, in order to avoid building a complex FEM model to extrapolate the hot-spot stress, empirical equations of the Stress Concentration Factor (SCF) can be used. Appropriate S-N design curves are then considered for fatigue life estimation. Some shortcomings of this approach when applied to welded tubular bridges including:

Copyright 2011 by the American Society of Civil Engineers

Accepted Manuscript
Not Copyedited

Journal of Bridge Engineering. Submitted October 25, 2010; accepted May 24, 2011;
posted ahead of print May 26, 2011. doi:10.1061/(ASCE)BE.1943-5592.0000274

- The bridge geometries may fall out of the validity range for the SCF equations, meaning an important effort to build a detailed numerical model of the joint in order to estimate the SCF of the joint under different service loading.
- The only parameters considered are the extrapolated structural stress range at the plate surface and the thickness of the potentially cracked plate. This tends to oversimplify the complexity of the joint geometry and does not differentiate among the different stress gradients through the plate thickness (Borges 2008)
- The HSS method is strictly only applicable to tubular joint *without* any surface crack and it cannot estimate the reminding fatigue life for a cracked tubular joint on any existing bridge. Once visible surface crack is observed on a tubular joint, the linear fracture mechanics should be employed for fatigue life re-estimation (Borges 2008, Lee et al. 2005)

The above reasons and the need for search of more realistic and economic (but safe) fatigue assessment procedure, especially for cracked structures, led the Steel Structures Laboratory (ICOM) of the EPFL and the School of Civil and Environmental Engineering of the NTU to carry out a collaborative research in this domain. The investigations which were carried out independently included both numerical and experimental studies. For numerical studies, two different methodologies were implemented and validated with the experiments. The first one is based on the Boundary Elements Method (BEM) code BEASY (BEASY 2003) and was implemented at EPFL in the framework of a study on size effects on the fatigue behavior of tubular joints (Borges 2008). The second one is based on the Finite Elements Method (FEM) code ABAQUS (ABAQUS 2006) and was implemented at NTU (Lie et al. 2001, Lee et al. 2005, Lie et al. 2005a, Lie et al, 2005b). In the following section, a brief description of the assumptions made to model a K-joint, for proper SIF determination is given. The modeling techniques are then briefly summarized.

Copyright 2011 by the American Society of Civil Engineers

Accepted Manuscript
Not Copyedited

Journal of Bridge Engineering. Submitted October 25, 2010; accepted May 24, 2011;
posted ahead of print May 26, 2011. doi:10.1061/(ASCE)BE.1943-5592.0000274

Joint elements

Figure 2 shows the geometry of a gapped CHS K-joint and the following parameters are used to characterize the joint:

$$\beta = {d_b}/{d_c} \qquad \gamma = {d_c}/{2t_c} \qquad \tau = {t_b}/{t_c} \qquad \alpha = {2L_c}/{d_c} \tag{0.1}$$

Both the EPFL and the NTU models consider the equations of cylinders intersection to derive the tubes geometry and intersections. In the current study, symmetry was not taken advantage of. This choice was made because it makes the current model more versatile and valuable for an extension of the present study to asymmetrical cracks.

Weld geometry

The weld geometry has a big influence on the stress concentration at the weld toe and thus on the stress intensity factors (SIF) for surface cracks. Therefore the welds should be modeled as close as possible to the reality. As it is a difficult task to simulate the weld profile realistically, most of previous investigations did not consider it. However, according to Lee and Wilmshurst (1995), an underestimation of the fatigue life up to 20% could result if the weld profile geometry is not modeled.

Furthermore, it should be mentioned that the welding residual stresses can be shown to be highly tensile (but still well below the yield stress of the material) in the zone between the braces (Acevedo and Nussbaumer 2009), a fortiori at the weld toe. The applied loading on the critical tubular joint is also tension in the chord and tension in the brace next to the cracking (joints under compression are less failure critical). Thus, the crack is always open, even under

Copyright 2011 by the American Society of Civil Engineers

Accepted Manuscript
Not Copyedited

Journal of Bridge Engineering. Submitted October 25, 2010; accepted May 24, 2011;
posted ahead of print May 26, 2011. doi:10.1061/(ASCE)BE.1943-5592.0000274

the minimum load; in other words, the cycles are fully effective, at least for a crack size up to half the chord wall thickness. Thus the SIF can be computed without consideration for the residual stresses, nor the applied stress ratio.

The EPFL weld geometry

In the EPFL model (Borges 2008), the weld was defined using the following three auxiliary curves for each brace-chord intersection (Figure 3)):

a. The intersection of the inner boundary of the diagonal with the chord outer boundary;

b. The intersection of the outer boundary of the diagonal with the chord, shifted by ($T_{W1}\cos(\theta_{br})$, 0, $T_{W1}\sin(\theta_{br})$);

c. The intersection of the chord with an imaginary cylinder with the same angle θ_{br} as the diagonal but a diameter equal to $d^* = d + 2\,T_{W2}$ and translated by (T_{W3}, 0, 0).

The model of the weld represents closely the real weld geometry and both respect the AWS or the AASHTO (AASHTO 2010) requirements (Nussbaumer et al. 2008).

The NTU weld geometry

In the NTU model, the weld model was defined differently but it is also complied with the AWS specifications (Lie et al. 2001). Figure 4 and Figure 5 show the basic geometry and the plan view for the weld path of a welded joint, respectively. The welded model is obtained by modifying the original inner and outer intersecting curves. The original contact thickness T_1 is defined as the thickness at a particular section normal to the intersection at the joint. To model the weld toe W_o, a shift of a distance T_2 from A_o is made (Figure 6). The equations for the outer intersecting curve (weld toe) can be written as (Lie et al. 2001):

Copyright 2011 by the American Society of Civil Engineers

Accepted Manuscript
Not Copyedited

Journal of Bridge Engineering. Submitted October 25, 2010; accepted May 24, 2011;
posted ahead of print May 26, 2011. doi:10.1061/(ASCE)BE.1943-5592.0000274

$$\begin{cases} Z_{W_O} = Z_{A_O} + T_2 \cos\beta_o \\ Y_{W_O} = Y_{A_O} + T_2 \sin\beta_o \\ X_{W_O} = \sqrt{R_1^2 - Y_{W_O}^2} \end{cases} \quad (0.2)$$

where $A_o(X_{A_O}, Y_{A_O}, Z_{A_O})$ is on the outer intersecting curve.

For the weld root is formed by shifting a distance T_3 being from A_i towards inside to get W_i (Figure 6) and the equations for the weld root can be expressed as (Lie et al. 2001)

$$\begin{cases} Z_{W_i} = Z_{A_i} + T_3 \cos\beta_o \\ Y_{W_i} = Y_{A_i} + T_3 \sin\beta_o \\ X_{W_i} = \sqrt{R_1^2 - Y_{W_i}^2} \end{cases} \quad (0.3)$$

where $A_i(X_{A_i}, Y_{A_i}, Z_{A_i})$ is on the inner intersecting curve.

The weld thickness T_W is defined as the sum of T_1, T_2 and T_3. Lie et al (2001) studied the actual welding thickness of full scale tubular T and Y joints and found that T_W their weld model provide consistent and reasonably conservative weld thickness predictions.

Crack geometry

When a crack initiates from the surface of the chord of a welded tubular joint, it will propagate through the chord thickness in a specific direction in which the energy requirement is minimal. The crack front will propagate on 3D curves which form the crack surface where the crack front lies on. The crack propagates along a critical plane which is normal to the principal stress or Von Mises' stress. This critical plane is difficult to find analytically as it involves finding the angle in which the stress is maximized. In the present study, the crack shape and critical plane are taken from experimental observations.

Stress analyses of the uncracked joint identified that the crown toe is where high stress concentration exists. Supported by experimental evidence (Schumacher, 2003, Borges, 2008),

Copyright 2011 by the American Society of Civil Engineers

Accepted Manuscript Not Copyedited

Journal of Bridge Engineering. Submitted October 25, 2010; accepted May 24, 2011;
posted ahead of print May 26, 2011. doi:10.1061/(ASCE)BE.1943-5592.0000274

only cracks starting at the crown toe are considered in the present study. In both FE and BE analyses, cracks are grown until they reach one half of the thickness. From this depth the boundary element model would need time consuming remeshing until the through thickness is attained. As most of the fatigue life is consumed during small crack stages, the half chord thickness crack depth can be considered a reasonable limit.

The EPFL crack surface model

The EPFL crack geometry is defined by the surface that contains both the weld toe (i.e. the intersection between the weld and the chord) and the crack front corresponding to the crown toe. The crack front is obtained by projecting a semi-ellipse over a conic surface whose directrix is the weld toe curve and the apex belongs to the *xoz* plane (Figure 7). The crack angle, ϕ_{crack}, determines the *x* coordinate of the apex. The crack faces belong to the conic surface and the crack front is doubly-curved (see Figure 8). This complex geometry makes modeling of the crack its propagation a complicated task.

The NTU crack model

In the NTU crack model, the surface is formed by joining a series of straight lines W_oD along the weld path (Figure 9). W_oD is passing through the Z-axis. $W_o(X_{W_o}, Y_{W_o}, Z_{W_o})$ is on the outer chord face. D is located on the inner chord face so that $\left|\overrightarrow{W_oD}\right| = t_C = R_1 - R_2$ and the line $\overrightarrow{W_oD}$ will pass through Z-axis (Lie et al., 2001). From full scale test results on the T, Y and K-joints (Lie et al., 2003, Chiew et al. 2004, Lie et al.2005b), it is known that the crack front shape resembles a semi-ellipse on a normalized u'-v' plane. Hence, the crack front equation is first defined on a normalized space and then map onto the crack surface (Figure 10, Lee et al. 2005).

Copyright 2011 by the American Society of Civil Engineers

Accepted Manuscript
Not Copyedited

Journal of Bridge Engineering. Submitted October 25, 2010; accepted May 24, 2011;
posted ahead of print May 26, 2011. doi:10.1061/(ASCE)BE.1943-5592.0000274

THE FE AND BE MODELS

Introduction

The estimation of a fatigue crack life using the theory of Linear Elastic Fracture Mechanics (LEFM) involves the calculation of stress intensity factors (SIF) at a number of discrete crack depths. Different methods can be used to estimate SIFs. Most of them involve the use of expressions deduced from parametric studies on specific geometry ranges. A more complex way involves advanced modelling of the crack by finite element or boundary element codes.

The finite element method has been widely used in fracture mechanics applications. Recent investigations applied the finite element method to simulate the crack behaviour in CHS joints (Shao, 2005). An intrinsic feature of the finite element method, common to all these formulations, is the need for continuous remeshing of the three-dimensional volume to follow the crack extension; this is a practical disadvantage of this method (Mellings et al., 2003).

In the boundary element method, only the boundary of the domain of interest is discretised (Hartmann, 1989). One disadvantage of this method is that it can only be used for linear elastic problems. However this is not an issue in modelling fatigue life in the long life region (the opposite from oligocyclic fatigue).

The EPFL BEM model

In order to create a boundary element model simulating a cracked uniplanar K-joint, different aspects have to be considered. Firstly, the geometry of the boundaries that define the joint elements and respective intersections have to be parameterized.

The crack path, or, in 3D, the surface defining crack faces, has also to be defined. A number of zones are created to confine regions of similar mesh density and material properties (Figure 11). The mesh discretizing the boundaries is chosen and the external forces and boundary

Copyright 2011 by the American Society of Civil Engineers

Accepted Manuscript
Not Copyedited

Journal of Bridge Engineering. Submitted October 25, 2010; accepted May 24, 2011;
posted ahead of print May 26, 2011. doi:10.1061/(ASCE)BE.1943-5592.0000274

conditions applied to mesh points. In the present study, the proportions of the joint elements may change and it is therefore very important to ensure that the results reflect the effect of size changes and not the effect of meshes being somewhat different. The following paragraphs describe the joint and crack meshing.

The BE model includes about 8100 mesh points and 2300 elements (total of about 30000 degrees of freedom) distributed in 8 zones as shown in Figure 11. Zones are groups of elements which can be considered as substructures of the component. Among these 8 zones, Zone 2 (Figure 11), where the crack is located and the stress is highly nonlinear, has a dense mesh (Figure 12); Zones 6, 7 and 8 are rigid rings for the external force introduction. An Excel Workbook was prepared to generate the mesh point coordinates, elements (including the weld profile and crack) and zones definitions. The entire model is meshed with reduced quadratic four-sided elements Q38 wherever possible and exceptionally with triangular quadratic elements. Tests have shown that these elements provide highly accurate solutions and reduce modeling time and disk requirements (BEASY, 2003). The mesh of the crack surface has to be carefully chosen. A good quality mesh depends on the shape of the elements defining the crack surface. The mesh points are calculated to suit the curved shape. BEASY automatically remeshes the area near the crack in order to optimally adapt the crack mesh within the existing joint mesh (see Figure 12).

Although BEASY software provides a crack growth tool allowing for automatic crack propagation from an initial crack, a manual, stepwise, crack modeling was preferred. The following reasons justify this option:

- due to the sharp weld toe geometry, automatic crack growth requires a very small step size so that the crack path remains at the weld toe;

Accepted Manuscript
Not Copyedited

Copyright 2011 by the American Society of Civil Engineers

Journal of Bridge Engineering. Submitted October 25, 2010; accepted May 24, 2011;
posted ahead of print May 26, 2011. doi:10.1061/(ASCE)BE.1943-5592.0000274

- the substantial amount of time spent to automatically grow a crack from a_0 to $T/2$ and the model sizes would have made it impossible to carry-out a parametric study in a reasonable amount of time;
- the need for identical crack path for the different basic load cases to make it possible to isolate/superpose their influence;
- manual crack growth allows the control of the crack shape, $a=c$, evolution and thus an indirect inclusion of the coalescence phenomenon;

The manual crack growth corresponds to the calculation of a set of models with built-in cracks of different given shapes and depths. The SIFs are computed using the crack opening displacement COD method (Cisilino and Aliabadi 2004). As in the case of FEM, extensive validation was carried out by comparison to alternative current potential drop (ACPD) (Lie 2005b) test results and mesh convergence tests were done (Borges, 2008).

The NTU FE model

In the NTU FE model, in order to ensure the quality of the final mesh, the whole tubular joint is always first divided into several zones before the mesh generation is started (Lie et al. 2001) Tailor-made programmes were created so that the meshes for different zones are generated independently (Figure 13). After the meshes of all the zones have been generated, they are then merged together to form the mesh of the entire structure. This approach makes it much easier to generate mesh with different grading in different zones. In order to save analysis time, small size elements will be created for the zones with high stresses while coarse mesh will be created at where low stress regions.

In order to obtain a good estimation of the SIF near the crack front, the mesh should be highly refined and of a high quality near crack mouth. In order to achieve such condition, five types of elements namely, tetrahedral, hexahedral, prism, pyramid and the quarter-point elements,

Copyright 2011 by the American Society of Civil Engineers

Accepted Manuscript
Not Copyedited

Journal of Bridge Engineering. Submitted October 25, 2010; accepted May 24, 2011;
posted ahead of print May 26, 2011. doi:10.1061/(ASCE)BE.1943-5592.0000274

which are available in the ABAQUS programme, were used to simulate a good quality mesh along the crack front (Lee et al. 2005 and Lie et al. 2003). Figure 14 shows different types of elements used to model a typical surface crack. A typical K-joint mesh normally consist of 20000 elements and 15000 nodes and the SIF values are obtained by using the well established and validated J-integral technique (Lee at al. 2005 and ABAQUS, 2006). The convergence, accuracy and the reliability of the NTU's mesh generation procedure developed had been validated extensively (Lie et al. 2003, 2005a and 2005b) and it is found that slightly conservative SIF values when compared with experimental measurement could be predicted in virtually all cases.

EVALUATION OF STRESS INTENSITY FACTORS

Introduction

In order to compare the results obtained using both techniques two cases were selected.

In Case 1, the joint is submitted to balanced brace axial load and is restrained in the chord extremities (see Figure 15) while in Case 2 the joint is under balanced axial load and bending moment (and one brace extremity is restrained, see Figure 19). Case 2 reproduces an experimental test carried out in NTU [Lie et al. 2005a, 2005b].

Table Table 1 and Table 2 show dimensions and the non-dimensional parameters for Case 1 and Case 2, respectively. For case 1 crack geometry "EPFL" (only BEM) and crack geometry "NTU" (BEM and FEM) were modeled and results compared. For case 2 only crack geometry "NTU" (BEM and FEM) was modeled. The analysis of case 1 explores the stress intensity factor results along the crack front, the influence of crack shape and geometry and the influence of the weld size while case 2 compares numerical results to experimental results and solutions from the literature at different crack depths.

Copyright 2011 by the American Society of Civil Engineers

Accepted Manuscript
Not Copyedited

Journal of Bridge Engineering. Submitted October 25, 2010; accepted May 24, 2011;
posted ahead of print May 26, 2011. doi:10.1061/(ASCE)BE.1943-5592.0000274

For the geometries and load cases considered, the SIF for opening mode 1, independent studies [Lee et al. 2005 and Borges 2008] show that K_I, are much larger than K_{II} and K_{III} for K-joints with a surface crack at the crown with effects of K_{II} and K_{III} could be ignored for practical purpose. Therefore, for simplicity, only results for K_I are presented. K_I from numerical results are directly compared to experimental SIF or Bowness's mixed mode SIF formulae (Lee and Bowness 2002) as the introduced error remains negligible compared to the precision of those measures.

Case 1: K-joint under balanced axial loads

Case 1 considers a K-joint with each of the brace lengths equal to 1610 mm, a chord length of 2100 mm, under balanced axial loadings (Figure 15). Both extremities of the chord are restrained. The gap clearance g is 40 mm. A semi-elliptical surface crack is placed at the weld toe crown. All the K_I results referring to Case 1 are normalized by dividing them by the nominal stress K_I/σ_{nom}.

Stress intensity factors at deepest point and crack tips

An initial crack depth a=10 mm and c=60 mm (a/T=0.5 and a/c = 0.167) is located at the crown. Table 3 compares the normalized stress intensity K_I/σ_{nom} factor results at the deepest point and the crack tips obtained using the Bowness equations (Lee and Bowness 2002) or the FEM and BEM methods as described in previous sections. Both FEM and BEM results converge while Bowness equations give a higher limit for this kind of joint. SIF at the crack tips tend to be 20 to 50% different than the values at the deepest point. This result has to be dealt with some caution as it may reflect a numerical perturbation linked to the mesh quality in this very sensitive area due to the singular geometry in the neighborhood as explained in the next paragraph.

Copyright 2011 by the American Society of Civil Engineers

Accepted Manuscript
Not Copyedited

Journal of Bridge Engineering. Submitted October 25, 2010; accepted May 24, 2011;
posted ahead of print May 26, 2011. doi:10.1061/(ASCE)BE.1943-5592.0000274

Stress intensity factors along the crack front for different crack shapes

Figure 16 shows the stress intensity factors along the crack front for different crack shapes keeping the crack depth constant and equal to 10mm or a/T=0.5. It is possible to observe that both the BE and FE model values are perturbed near the crack tips (i.e. extremities) and not always with the same tendency. This wave is believed to be due to the singular geometry at these points and also due to the fact the mesh is relatively coarse and not designed specifically to fit this areas (as for simple fatigue life calculation the deepest point is usually sufficient) and possibly due to the fact that at crack tips the semi-elliptical crack shape is not so adapted to simulate reality (i.e. the coalescence phenomenon). In order to increase the reliability and accuracy of these results, a mesh refinement is suggested. Results at crack tips require a finer mesh and are less reliable than the results at deepest point for equivalent meshes due to the singular geometry point at crack tips (resulting from curved intersection of 3 curved surfaces). This numerical problem raises doubts on the feasibility of automatic crack propagation using increment-wise routines to propagate the crack automatically as the following increment will reflect the perturbed results at the previous step and this can lead to no convergence issues or unreal crack propagations. Furthermore, and as expected, Figure 16 shows that as the crack shape ratio a/c decreases, the stress intensity values increase at the deepest point and decrease at the crack tips.

Stress intensity factors along the crack front at different crack depths

Figure 17 shows the SIF results along the crack front observed when keeping the crack length c = 60 mm constant, and considering different depth a. Stress intensity factor results for BEM models with the considered mesh can be obtained for a crack, at most, deep as $T/2$. For deeper cracks numerical problems arise, linked to the ratio between the elements size and the distance

Copyright 2011 by the American Society of Civil Engineers

Accepted Manuscript
Not Copyedited

between the boundary elements. If results were needed for deeper SIFs then the mesh would have to be refined both for tube and crack boundary elements. These results show a good agreement between BE and FE models. In this case as the crack length is kept constant, the SIF values increase with the crack depth. The SIF at the crack tips increase more than the SIFs at the deepest point as a consequence of the a/c is increasing with a (c is constant).

Influence of weld sizes and crack geometries

Given a defined geometry, the assumptions to define the weld and crack geometry/shape were made independently at NTU and EPFL. A sensitivity analysis using BE models allows for an estimation of the influence of the "modeler" judgment when compared to the influence of measurable/objective/univocal geometric parameters such as weld size. To understand the influence of the crack geometry, both EPFL and NTU crack geometries were modeled using BEM. Comparison of results for EPFL crack and NTU crack geometries (when modeled in BEM) are shown in Figure 18. Different additional models with variable weld sizes are also plotted for comparison of the differences obtained when the crack shape and weld geometry are not explicitly given or have to be estimated. Comparison shows that the weld size can play a role as important as crack geometry. These can be associated to the "modeler" judgment influence – thus the "modeler" influence being estimated as about 35%. This value is in the range of precision of simplified methods such as Bowness and Lee.

Case 2: K-joint under balanced axial loads and bending moment

Case 2 reproduces the joint tested at NTU for which extensive ACPD results are available (Lie 2005b). The braces angle is 45º. In this case only one brace is loaded while the other one is restrained (see Figure 19).

Copyright 2011 by the American Society of Civil Engineers

Accepted Manuscript
Not Copyedited

Journal of Bridge Engineering. Submitted October 25, 2010; accepted May 24, 2011;
posted ahead of print May 26, 2011. doi:10.1061/(ASCE)BE.1943-5592.0000274

Influence of weld sizes

Figure 20 shows the SIF results for BE (respectively with weld size 6 and 7, see Table 4) and FE models. The three model results compare well, the differences being bigger on the crack tip neighborhood.

Comparison with experimental results

In order to reproduce the crack propagation at defined crack depths and compare SIF values to experimental values, the crack shapes for the corresponding crack depths are taken from experimental evidence [Lie 2005b] (see Figure 21) and reproduced numerically. When compared to experimental results (see Figure 22), Lee & Bowness (2002) SIFs for this type of joint are up to 40% higher, leading to very conservative estimations of the fatigue crack propagation life (less than half the measured lives). BE and FE results are also higher than the experimental values but a good agreement is found between these. Noted that the experimental curve should be seen as indicative and not as an exact curve. Measures in different joints would lead to different values with variations up to 20% (Borges 2008), even when the macroscopic geometry and loading conditions and measuring instrumentation are similar. This is due to the influence of random factors involved in crack nucleation such as the steel grain or the welding flaws that lead to different crack angles and shapes.

Comparison between the BE and FE Models

The presented models are compatible and lead to similar results which are also very close to experimentally measured values. Both techniques present advantages and disadvantages. If on one hand the meshing effort in BEM is less than for FEM. On the other hand FEM models provide through thickness stress/strain results and the possibility to consider non-linear

Copyright 2011 by the American Society of Civil Engineers

Accepted Manuscript
Not Copyedited

Journal of Bridge Engineering. Submitted October 25, 2010; accepted May 24, 2011;
posted ahead of print May 26, 2011. doi:10.1061/(ASCE)BE.1943-5592.0000274

behavior. The strategy developed at NTU is more flexible in terms of mesh generation (FEM), becoming easier for the modeler to refine or change the mesh grade. The generally accepted advantages of BEM for LEFM against FEM are limited in the case of tubular structures (the thinner the tubes the more penalized the BEM would be) since the elements size is a function of the minimum distance between boundaries. BEM would be more advantageous for massive pieces as "cubes" or "spheres", where the FEM has to mesh the volume and BEM has to model only the surfaces and not necessarily with fine mesh as the distance between opposite boundaries is relatively big.

SUMMARY AND CONCLUSIONS

The present paper discusses two different techniques to simulate welded CHS K-joint cracking: FEM and BEM. The numerical results obtained shown that both techniques give similar results when modeling is properly done. In terms of modelling effort needed, it was found that meshing of model and crack, in particular when its geometry is curved, is more difficult in FEM than in the BEM. However, advantages of FEM include meshing versatility once tools for modeling were created and the possibility to include non-linear behavior straight forward.

More importantly, the numerical results obtained from both models are consistent with the experimental data and with each other. Furthermore, both modelling techniques lead to lower and better estimations of SIF when comparing with those conservative formulas (Lee and Bowness 2002) and this implies that more accurate fatigue life estimation could be obtained if such advance modelling procedures, which is currently outside the standard design code requirement (CIDECT 2001, AASHTO 2010 and AWS 2008) are employed in practice. Moreover, the numerical results also highlighted the influence of major geometrical parameters and the modelling assumptions adopted by the modeler. In particular, it is shown

Copyright 2011 by the American Society of Civil Engineers

Accepted Manuscript
Not Copyedited

Journal of Bridge Engineering. Submitted October 25, 2010; accepted May 24, 2011;
posted ahead of print May 26, 2011. doi:10.1061/(ASCE)BE.1943-5592.0000274

that the modeler preference is could influence the results by up to 35%, especially near the crack trips. However, it should be noted that this value is in the range of precision of simplified methods (Lee and Bowness 2002). Finally, it is also found that the reliability quality of the SIF at the deepest crack depth is much better than at near the crack tips. This fact raises doubts over the accuracy and practical feasibility of automatic propagation tools.

AKNOWLEDGEMENTS

The first author would like to acknowledge the funding assistance provided by the Swiss National Science Foundation (SNF) for his PhD study and the School of Civil and Environmental Engineering, NTU for his academic visit to NTU, Singapore, in February 2009.

Accepted Manuscript
Not Copyedited

Copyright 2011 by the American Society of Civil Engineers

Journal of Bridge Engineering. Submitted October 25, 2010; accepted May 24, 2011;
posted ahead of print May 26, 2011. doi:10.1061/(ASCE)BE.1943-5592.0000274

REFERENCES

AASHTO/AWS D1.5M/D1.5:2010, Bridge Welding Code, 6th Edition, American Association of State Highway and Transportation Officials. 444 N Capitol St. NW - Suite 249 - Washington, DC 20001

ABAQUS (2006), User Manual (Ver. 6.5), Hibbit, Karlsson and Sorensen Inc., USA.

Acevedo C. and Nussbaumer A. (2009). Residual stress estimation of welded tubular K-joints under fatigue loads. Proceedings of the 12th International Conference on Fracture. Ottawa 2009

American Welding Society, AWS, (2008), ANSI/AWS D1.1/D1.1M-2008 Structural Welding Code-Steel, Miami, USA

BEASY User Guide, (2003) Computational mechanics BEASY Ltd, Ashurst, Southhampton

Borges, L. C., "Size Effects in the Fatigue Behaviour of Tubular Bridge Joints". PhD Thesis no. 4142, Ecole Polytechnique Fédérale de Lausanne (EPFL), 2008.

CIDECT (2001), Design Guide 8, For CHS and RHS welded joints under fatigue loading. CIDECT, TÜV Verlag, Köln CIDECT

Cisilino, A P., Aliabadi, M. H., "Dual boundary element assessment of three-dimensional fatigue crack growth", Engineering Analysis with Boundary Elements, Volume 28, Issue 9, September 2004, Pages 1157-1173

Chiew, S. P., Lie, S. T., Lee, C. K., Huang Zhiwei, (2004), "Fatigue Performance of Cracked Tubular T Joints under Combined Loads. I: Experimental", ASCE Journal of Structural Engineering. Vol. 130, No. 4, pp 562 - 571.

Eekhout M., (1991) "Tubular and Glass Structures". In Tubular structures: The 4th International Symposium Delft, pp. 148–173. Delft University Press, 1991.

Copyright 2011 by the American Society of Civil Engineers

Accepted Manuscript
Not Copyedited

Hartmann, F. "Introduction to boundary elements" Springer-Verlag, 1989. ISBN 3-540-50430-3.

Karamanos, S.A., Romeijn, A. and Wardenier, J., (2000), "Stress concentrations in tubular gap K-joints: mechanics and fatigue design". Engineering Structures, pp. 4-14.

Lee, M. M. K., Bowness, D. (2002) "Estimation of stress intensity factor solutions for weld toe cracks in offshore tubular joints", International Journal of Fatigue, Volume 24, Issue 8, August 2002, Pages 861-875.

Lee, C. K., Lie, S. T., Chiew, S. P., Shao Yongbo, (2005), "Numerical models verification of cracked tubular T, Y and K-joints under combined loads", Engineering Fracture Mechanics. Vol. 72, No. 7, pp 983 - 1009.

Lee, M. M. K., Wilmshurst, S. R. (1995) "Numerical modelling of CHS joints with multiplanar double-K configuration" Journal of Constructional Steel Research, 32(3):281–301.

Lie, S. T., Lee, C. K. and Wong S. M., (2001), "Modelling and mesh generation of weld profile in tubular Y-joint", Journal of Constructional Steel Research. Vol. 57, No. 5, pp 467 - 580.

Lie, S. T., Lee, C. K. and Wong S. M., (2003), "Model and mesh generation of cracked tubular Y-joints", Engineering Fracture Mechanics. Vol. 70, No. 2, pp 161 - 184.

Lie, S.T., Lee, C.K., Chiew, S.P. and Shao, Y.B., (2005a), "Mesh modeling and analysis of cracked uni-planar tubular K-joints". Journal of Constructional Steel Research, pp. 235-264

Lie, S. T., Lee, C. K., Chiew, S. P., Shao Yongbo, (2005b), "Validation of surface crack stress intensity factors of a tubular K-joint", International Journal of Pressure Vessels and Piping. Vol. 82, No. 8, pp 610 - 617.

Marshall, P., (1992), "Design of welded tubular connections, Basis and use of AWS provisions". Elsevier Science Publishers, Amsterdam

Copyright 2011 by the American Society of Civil Engineers

Accepted Manuscript
Not Copyedited

Mellings, S., Baynham, J., Adey, R. A. and Curtin, T. Durability prediction using automatic crack growth simulation in stiffened panel structures. Structures and Materials, 12:193–202, 2003.

Schumacher, A. (2003) "Fatigue behaviour of welded circular hollow section joints in bridges". PhD thesis no. 2727, Swiss Federal Institute of Technology (EPFL), Lausanne, 2003.

Schumacher, A., Nussbaumer, A., (2006), "Experimental study on the fatigue behavior of welded tubular k-joints for bridges", Engineering Structures, Vol. 28, pp. 745-755

Schumacher, A., Borges, L., Nussbaumer, A. (2009) "A critical examination of the size effect correction for welded steel tubular joints", International Journal of Fatigue, Elsevier Ltd. vol. 31, 2009, pp. 1422-1433

Shao, Y. (2005) Fatigue behaviour of uniplanar CHS gap k-joints under axial and in-plane bending loads". Ph.D. thesis, Nanyang Technological University. School of Civil and Environmental Engineering, 2005.

Accepted Manuscript
Not Copyedited

Copyright 2011 by the American Society of Civil Engineers

Journal of Bridge Engineering. Submitted October 25, 2010; accepted May 24, 2011;
posted ahead of print May 26, 2011. doi:10.1061/(ASCE)BE.1943-5592.0000274

TABLES

Table 1. Geometry parameters for the joints analysed.

	d_c [mm]	d_b [mm]	t_c [mm]	t_b [mm]	e [mm]	g [mm]	L_c [mm]	H [mm]	θ [º]
Case 1	273.0	139.7	20.0	12.5	54	58.7	2100	1780	60
Case 2	273.1	141.3	25.4	19.1	0	73.3	5911	3459	45

Table 2. Non-dimensional parameters for Case 1 and Case 2 geometries.

	β [-]	γ [-]	τ [-]	α [-]
Case 1	0.5	6.8	0.63	15.4
Case 2	0.5	5.4	0.75	43.3

Table 3. Comparison of normalized SIFs results at the deepest point and at the crack tips (a=10 mm and c=60 mm).

	SIFs at deepest point	SIFs at crack tips
	mm1/2	mm1/2
Lee & Bowness (2002)	13.5	20.1
FEM (DE*)	9.0	11.3
FEM (J-integral)	8.6	13.1
BEM (COD)	9.4	7.5 and 9.0

* Displacement Extrapolation

Table 4. Weld size definitions.

Weld size ID	T_{W1} [mm]	T_{W2} [mm]	T_{W3} [mm]	$\theta_{w,ch}$ [°]
Weld size 0	15.0	12.0	8.0	44
Weld size 1	10.0	6.7	3.3	43
Weld size 2	8.0	5.3	2.7	43
Weld size 3	6.0	4.0	2.0	43
Weld size 6	22.0	19.0	4.0	22
Weld size 7	25.0	22.0	5.0	22

Accepted Manuscript
Not Copyedited

Copyright 2011 by the American Society of Civil Engineers

Journal of Bridge Engineering. Submitted October 25, 2010; accepted May 24, 2011;
posted ahead of print May 26, 2011. doi:10.1061/(ASCE)BE.1943-5592.0000274

Nomenclature

a Crack depth in the middle, symmetry plane, along the crack face of different stages in process of crack propagation

c Half crack length measured along the weld toe

Cr Point along the crack front

C Material constant

d Depth of deepest point

d_b Thickness of reference brace

D Point on the inner chord surface

E Plane stress elastic modulus

$\overline{E}$ Plane strain elastic modulus

F Axial load

G Shear modulus

J J-integral

K_I Mode I stress intensity factor

K_{II} Mode II stress intensity factor

K_{III} Mode III stress intensity factor

K_e Equivalent stress intensity factor

ΔK Stress intensity factor range

m Material constant

M_i In-plane bending moment

N Number of cycles of cyclic load

R_1 Chord outer radius

R_2 Chord inner radius

Accepted Manuscript
Not Copyedited

Copyright 2011 by the American Society of Civil Engineers

Journal of Bridge Engineering. Submitted October 25, 2010; accepted May 24, 2011;
posted ahead of print May 26, 2011. doi:10.1061/(ASCE)BE.1943-5592.0000274

SCF	Stress concentration factor
u_r	Radial displacement
v_n	Normal displacement
w_t	Tangential displacement
t_b	Brace thickness
t_c	Chord thickness
T	Main plate or chord thickness
T_{wi}	Weld definition parameters
X_D	x-coordinate of a point on a circle
W_o	Point on the weld profile
X_D	x-coordinate of a point on a circle
Y_D	y-coordinate of a point on a circle
X_{Cr}	x-coordinate of a point along the crack front
Y_{Cr}	y-coordinate of a point along the crack front
Z_{Cr}	z-coordinate of a point along the crack front
X_{Wo}	x-coordinate of a point of the weld profile
Y_{Wo}	y-coordinate of a point of the weld profile
Z_{Wo}	z-coordinate of a point of the weld profile
β	Ratio of brace diameter to chord diameter
ρ	A given unknown
τ	Ratio of brace thickness to chord thickness
ϕ	Angle along the crack front

Accepted Manuscript
Not Copyedited

Copyright 2011 by the American Society of Civil Engineers

Journal of Bridge Engineering. Submitted October 25, 2010; accepted May 24, 2011;
posted ahead of print May 26, 2011. doi:10.1061/(ASCE)BE.1943-5592.0000274

Figures captions list

Figure 1. *Cais das Pedras* viaduct (1997, Porto - Portugal).

Figure 2**.** Geometric dimensions defining K-joint made of CHS.

Figure 3. Weld geometry according to EPFL model.

Figure 4. Definition and geometry of a welded tubular Y-joint

Figure 5. Inner and outer intersecting curves with the weld path

Figure 6. Enlarged view of geometry and modeling of the weld path.

Figure 7. A K-joint surface crack geometry definition.

Figure 8. K-joint surface crack mesh (BEM).

Figure 9. Formation of cracked surface in the chord thickness according to NTU model.

Figure 10. Mapping of 2D normalized plane to a 3D cracked surface

Figure 11. Boundary Model zones.

Figure 12. K-joint surface crack mesh detail (BEM).

Figure 13. Finite element mesh of cracked K-joint.

Figure 14. Different types of elements used to model the surface crack.

Figure 15. A K-joint under balanced axial loadings (Case 1).

Figure 16. SIF along the crack front of K-joints with crack depth a=10 mm being kept constant. a) a/c=0.50 ; a= 0.5 T ; b) a/c=0.25 ; a= 0.5 T; c) a/c=0.16 ; a= 0.5 T

Figure 17. SIF along the crack front of K-joints with crack depth c=60 mm being kept constant. a) a/T=0.30 ; c= 60mm ; b) a/T=0.50 ; c= 60mm

Figure 18. Comparison of the relative influence of the "modeller" vs. the weld size. (*Case 1:* a/T=0.50 ; c= 60mm)

Figure 19. A K-joint under bending and axial loadings (Case 2).

Figure 20. SIF along crack front for a/T = 0.53; a = 13.5 mm; c = 63 mm.

Figure 21. Relationship between crack shape a/c and relative crack depth a/T used in numerical modeling (from experimental measures).

Figure 22. Comparison between the numerical and experimental SIF values for the second K-joint specimen.

Accepted Manuscript
Not Copyedited

Copyright 2011 by the American Society of Civil Engineers

Fig 1

Journal of Bridge Engineering. Submitted October 25, 2010; accepted May 24, 2011;
posted ahead of print May 26, 2011. doi:10.1061/(ASCE)BE.1943-5592.0000274

Accepted Manuscript
Not Copyedited

Copyright 2011 by the American Society of Civil Engineers

Fig 2

Journal of Bridge Engineering. Submitted October 25, 2010; accepted May 24, 2011;
posted ahead of print May 26, 2011. doi:10.1061/(ASCE)BE.1943-5592.0000274

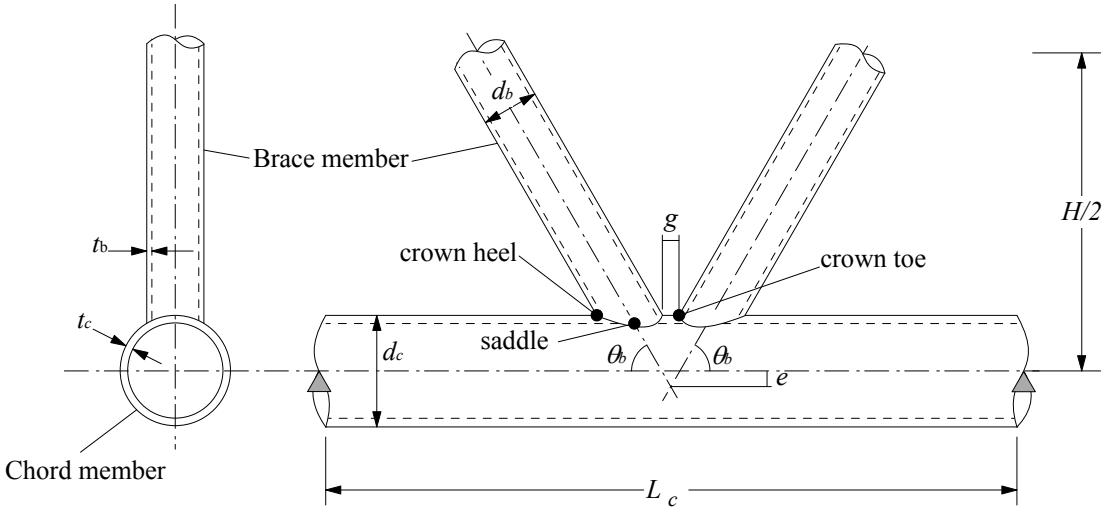

Accepted Manuscript
Not Copyedited

Copyright 2011 by the American Society of Civil Engineers

Fig 3

Journal of Bridge Engineering. Submitted October 25, 2010; accepted May 24, 2011;
posted ahead of print May 26, 2011. doi:10.1061/(ASCE)BE.1943-5592.0000274

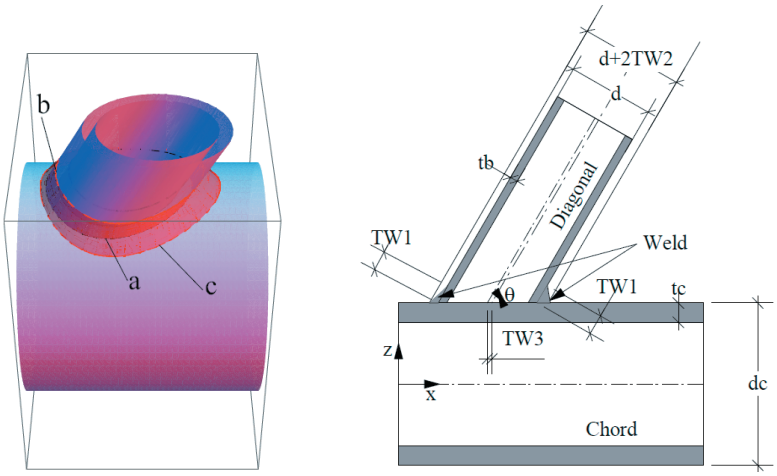

Accepted Manuscript
Not Copyedited

Copyright 2011 by the American Society of Civil Engineers

Fig 4

Journal of Bridge Engineering. Submitted October 25, 2010; accepted May 24, 2011;
posted ahead of print May 26, 2011. doi:10.1061/(ASCE)BE.1943-5592.0000274

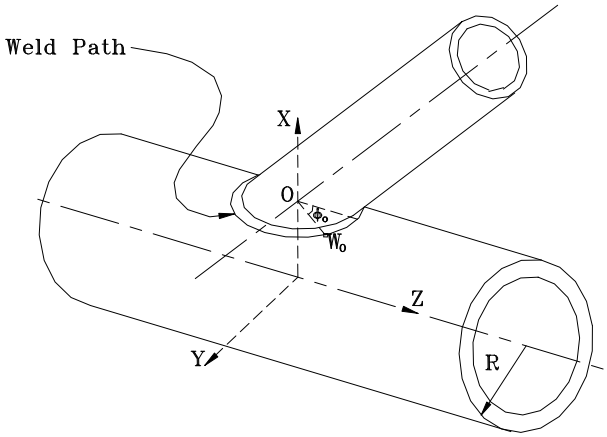

Accepted Manuscript
Not Copyedited

Copyright 2011 by the American Society of Civil Engineers

Fig 5

Journal of Bridge Engineering. Submitted October 25, 2010; accepted May 24, 2011;
posted ahead of print May 26, 2011. doi:10.1061/(ASCE)BE.1943-5592.0000274

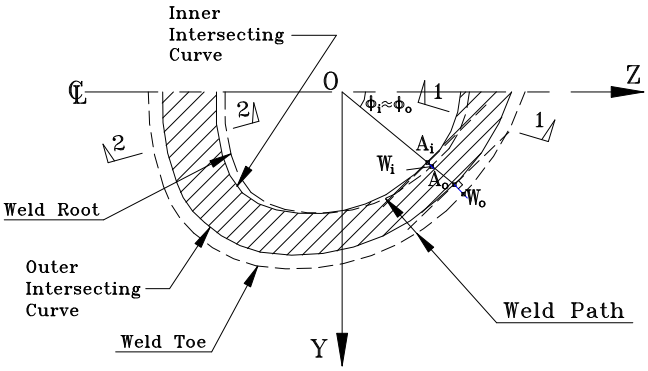

Accepted Manuscript
Not Copyedited

Copyright 2011 by the American Society of Civil Engineers

Fig 6

Journal of Bridge Engineering. Submitted October 25, 2010; accepted May 24, 2011;
posted ahead of print May 26, 2011. doi:10.1061/(ASCE)BE.1943-5592.0000274

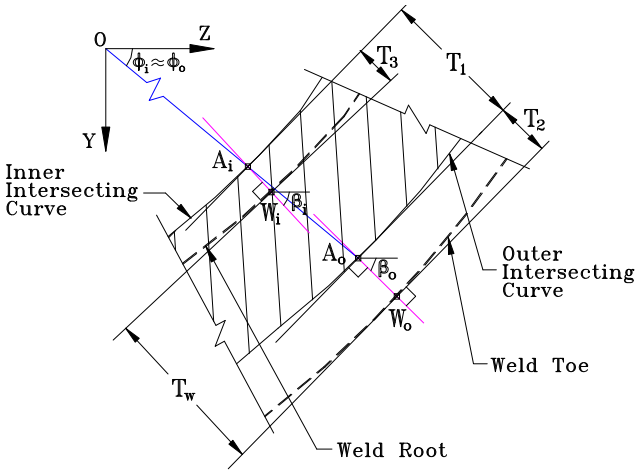

Accepted Manuscript
Not Copyedited

Copyright 2011 by the American Society of Civil Engineers

Fig 7

Journal of Bridge Engineering. Submitted October 25, 2010; accepted May 24, 2011;
posted ahead of print May 26, 2011. doi:10.1061/(ASCE)BE.1943-5592.0000274

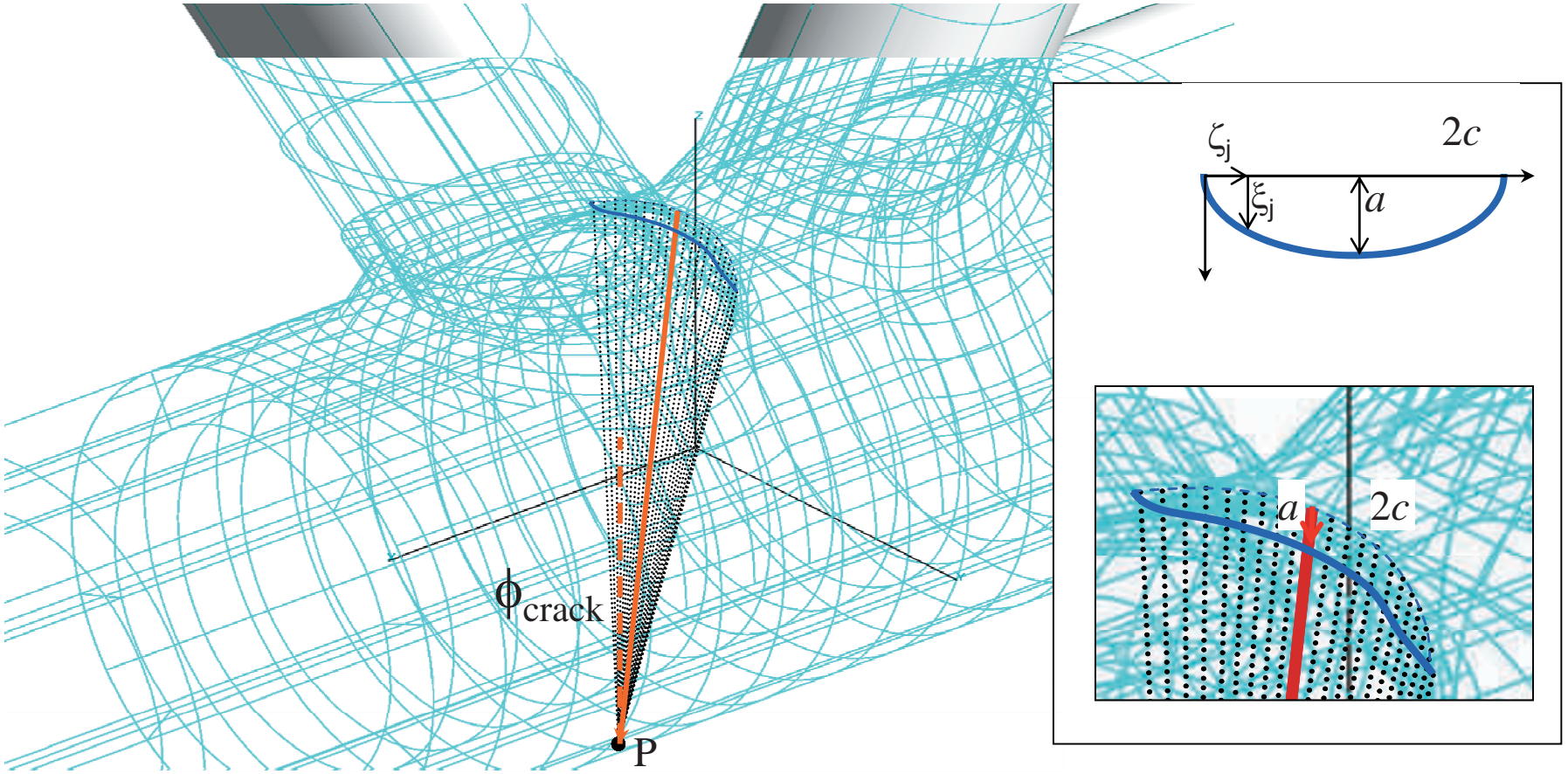

Accepted Manuscript
Not Copyedited

Copyright 2011 by the American Society of Civil Engineers

Fig 8

Journal of Bridge Engineering. Submitted October 25, 2010; accepted May 24, 2011;
posted ahead of print May 26, 2011. doi:10.1061/(ASCE)BE.1943-5592.0000274

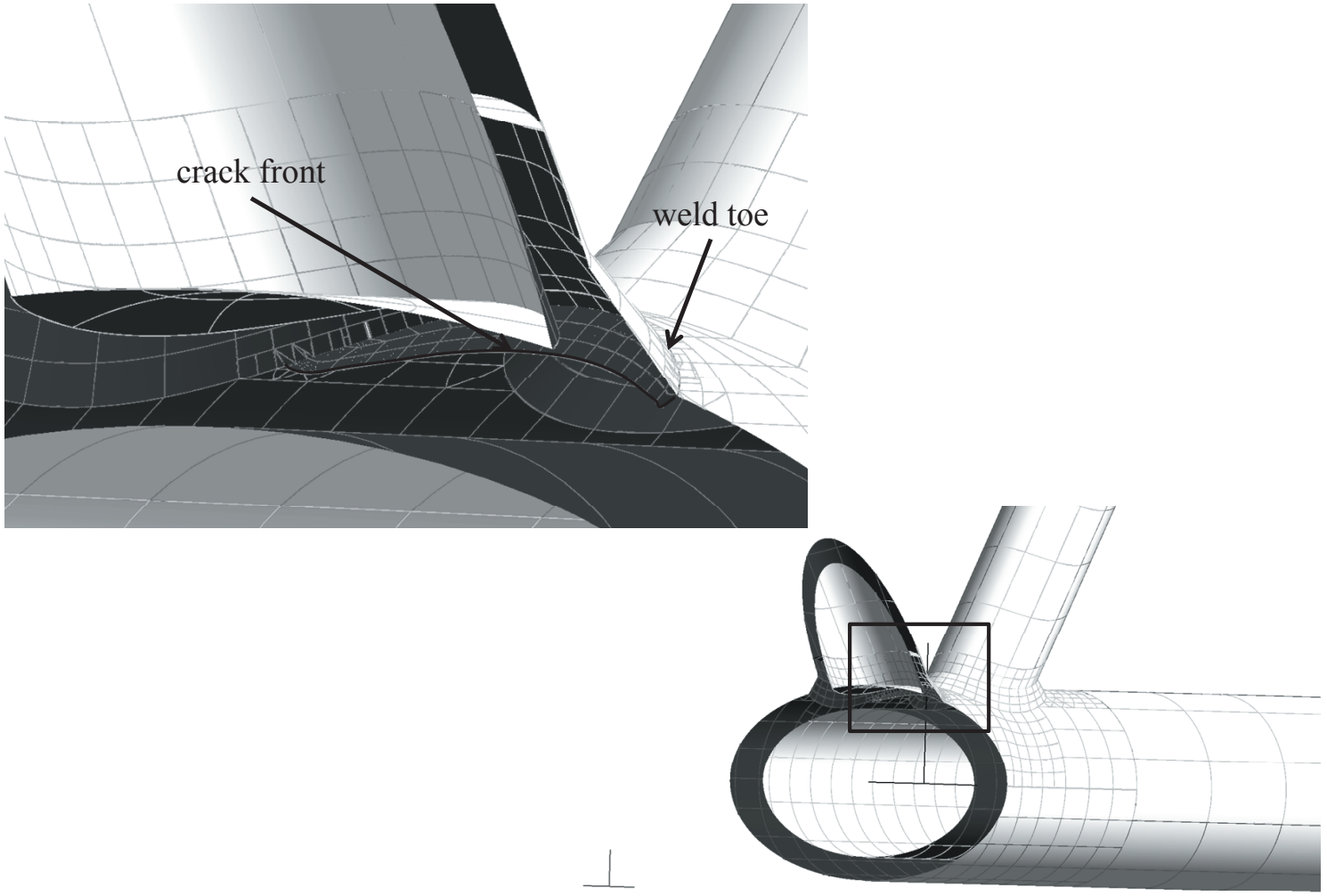

Accepted Manuscript
Not Copyedited

Copyright 2011 by the American Society of Civil Engineers

Fig 9

Journal of Bridge Engineering. Submitted October 25, 2010; accepted May 24, 2011;
posted ahead of print May 26, 2011. doi:10.1061/(ASCE)BE.1943-5592.0000274

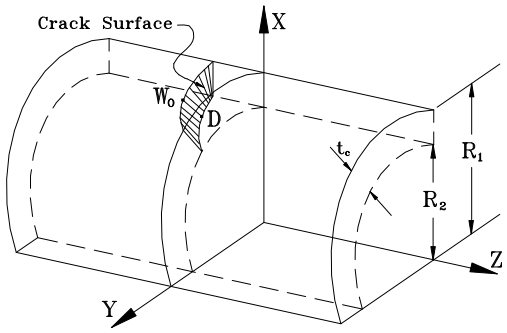

Accepted Manuscript
Not Copyedited

Copyright 2011 by the American Society of Civil Engineers

Fig 10

Journal of Bridge Engineering. Submitted October 25, 2010; accepted May 24, 2011;
posted ahead of print May 26, 2011. doi:10.1061/(ASCE)BE.1943-5592.0000274

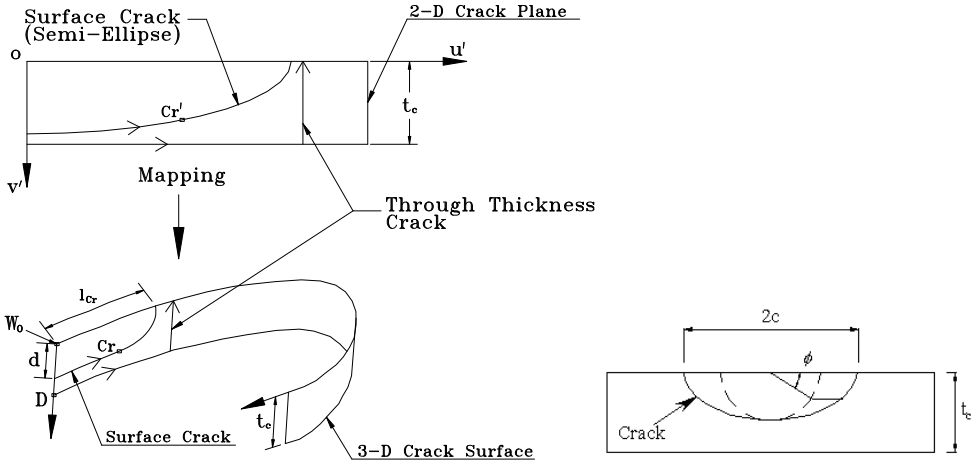

Accepted Manuscript
Not Copyedited

Copyright 2011 by the American Society of Civil Engineers

Fig 11

Journal of Bridge Engineering. Submitted October 25, 2010; accepted May 24, 2011;
posted ahead of print May 26, 2011. doi:10.1061/(ASCE)BE.1943-5592.0000274

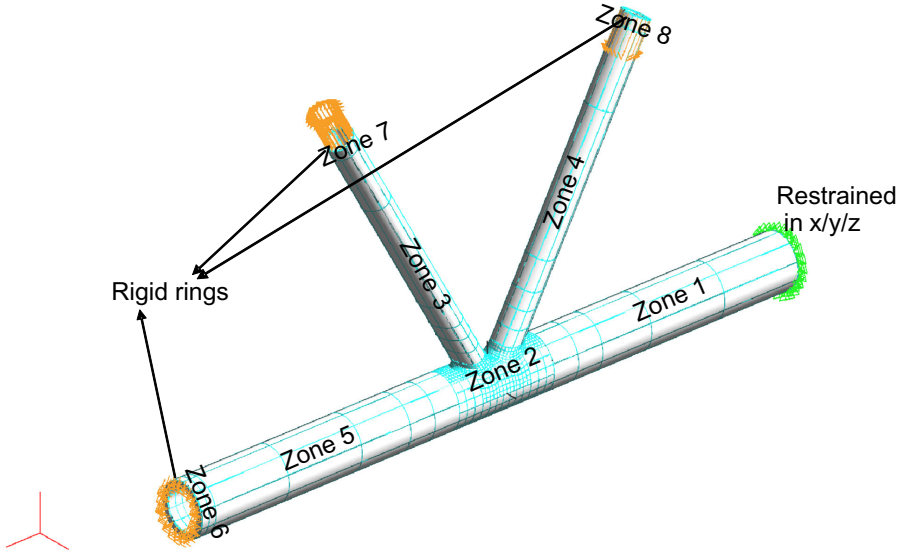

Accepted Manuscript
Not Copyedited

Copyright 2011 by the American Society of Civil Engineers

Fig 12

Journal of Bridge Engineering. Submitted October 25, 2010; accepted May 24, 2011;
posted ahead of print May 26, 2011. doi:10.1061/(ASCE)BE.1943-5592.0000274

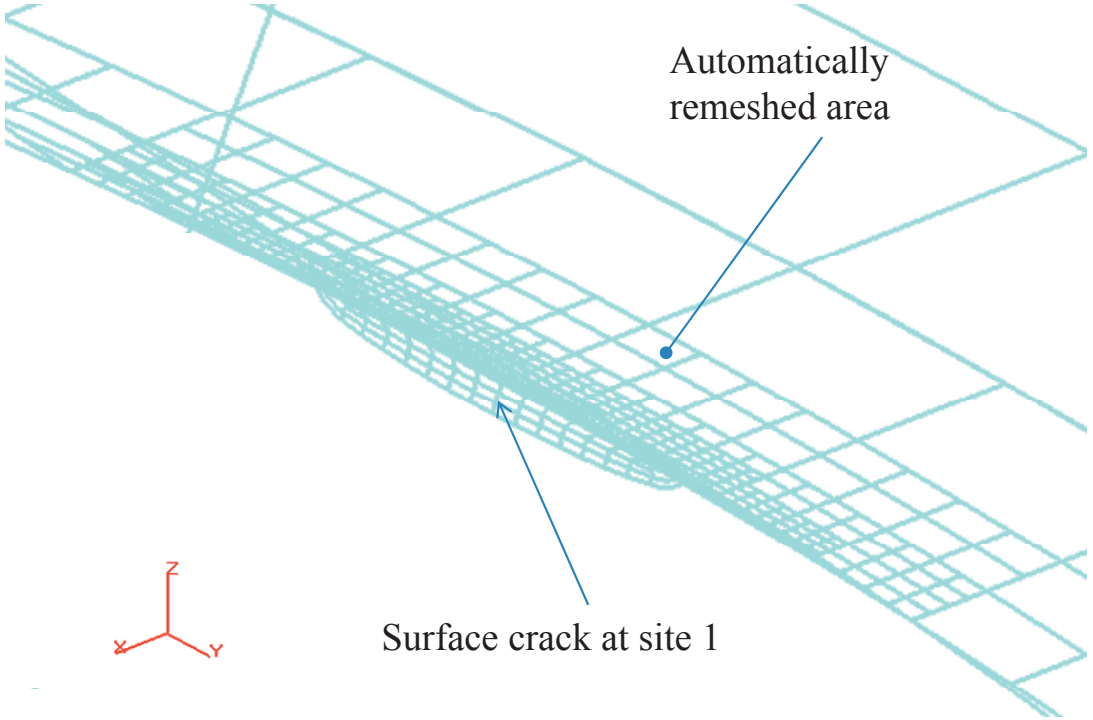

Accepted Manuscript
Not Copyedited

Copyright 2011 by the American Society of Civil Engineers

Fig 13

Journal of Bridge Engineering. Submitted October 25, 2010; accepted May 24, 2011;
posted ahead of print May 26, 2011. doi:10.1061/(ASCE)BE.1943-5592.0000274

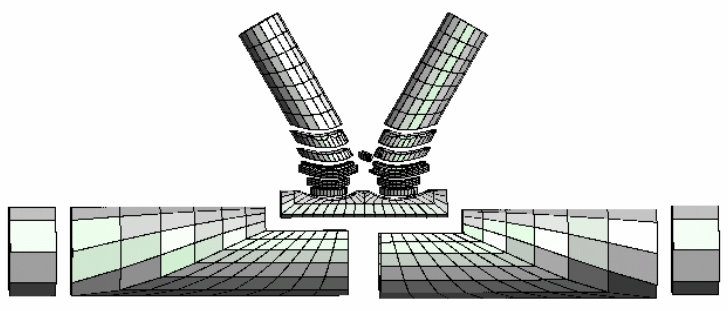

Accepted Manuscript
Not Copyedited

Copyright 2011 by the American Society of Civil Engineers

Fig 14

Journal of Bridge Engineering. Submitted October 25, 2010; accepted May 24, 2011;
posted ahead of print May 26, 2011. doi:10.1061/(ASCE)BE.1943-5592.0000274

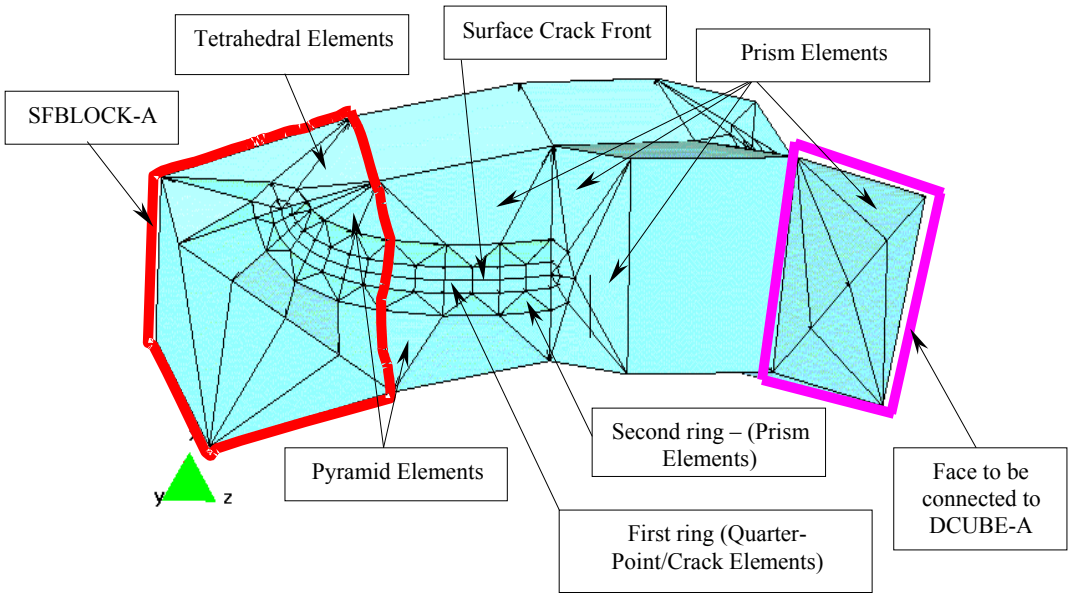

Accepted Manuscript
Not Copyedited

Copyright 2011 by the American Society of Civil Engineers

Fig 15

Journal of Bridge Engineering. Submitted October 25, 2010; accepted May 24, 2011;
posted ahead of print May 26, 2011. doi:10.1061/(ASCE)BE.1943-5592.0000274

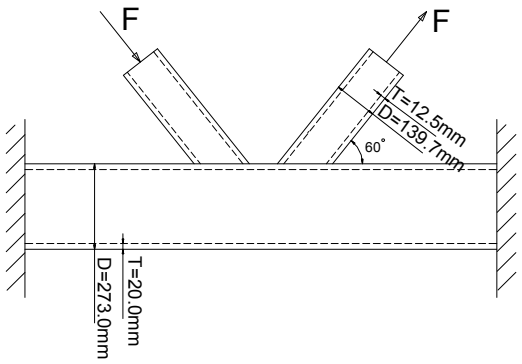

Accepted Manuscript
Not Copyedited

Copyright 2011 by the American Society of Civil Engineers

Fig 16

Journal of Bridge Engineering. Submitted October 25, 2010; accepted May 24, 2011;
posted ahead of print May 26, 2011. doi:10.1061/(ASCE)BE.1943-5592.0000274

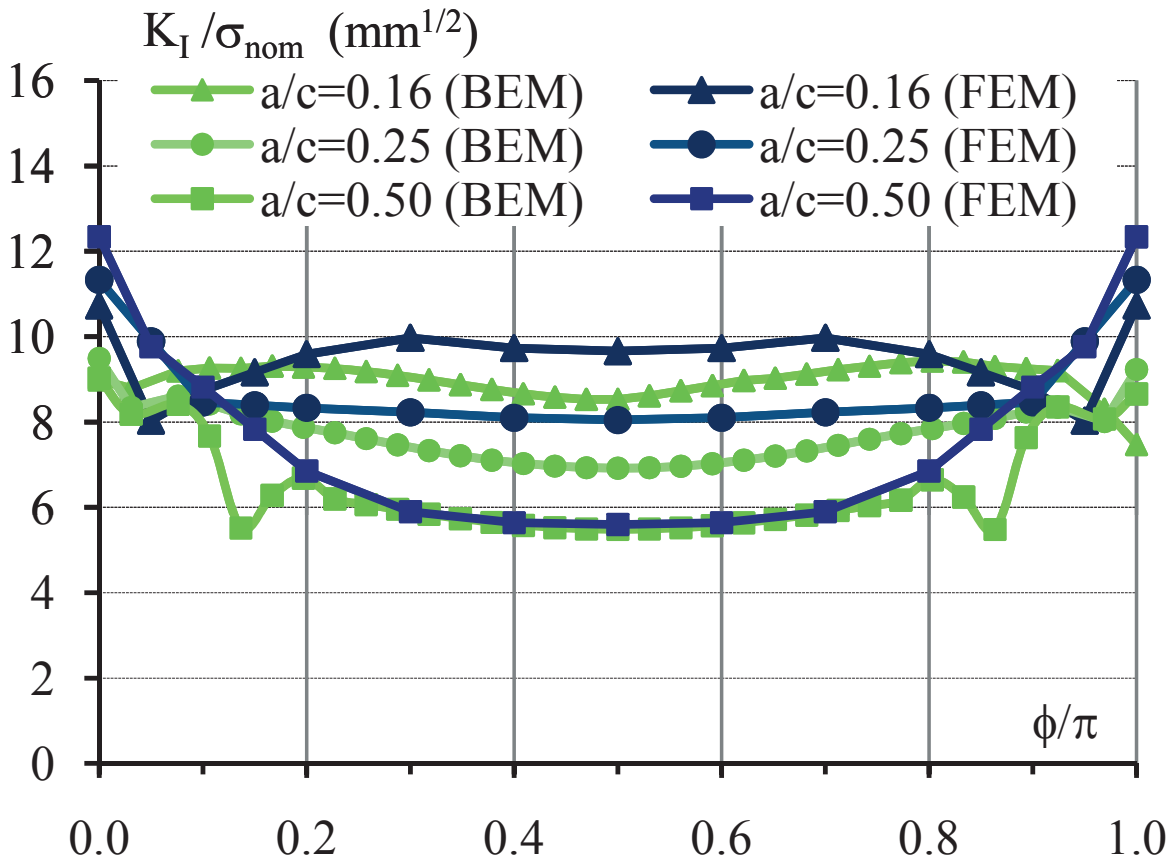

Accepted Manuscript
Not Copyedited

Copyright 2011 by the American Society of Civil Engineers

Fig 17

Journal of Bridge Engineering. Submitted October 25, 2010; accepted May 24, 2011;
posted ahead of print May 26, 2011. doi:10.1061/(ASCE)BE.1943-5592.0000274

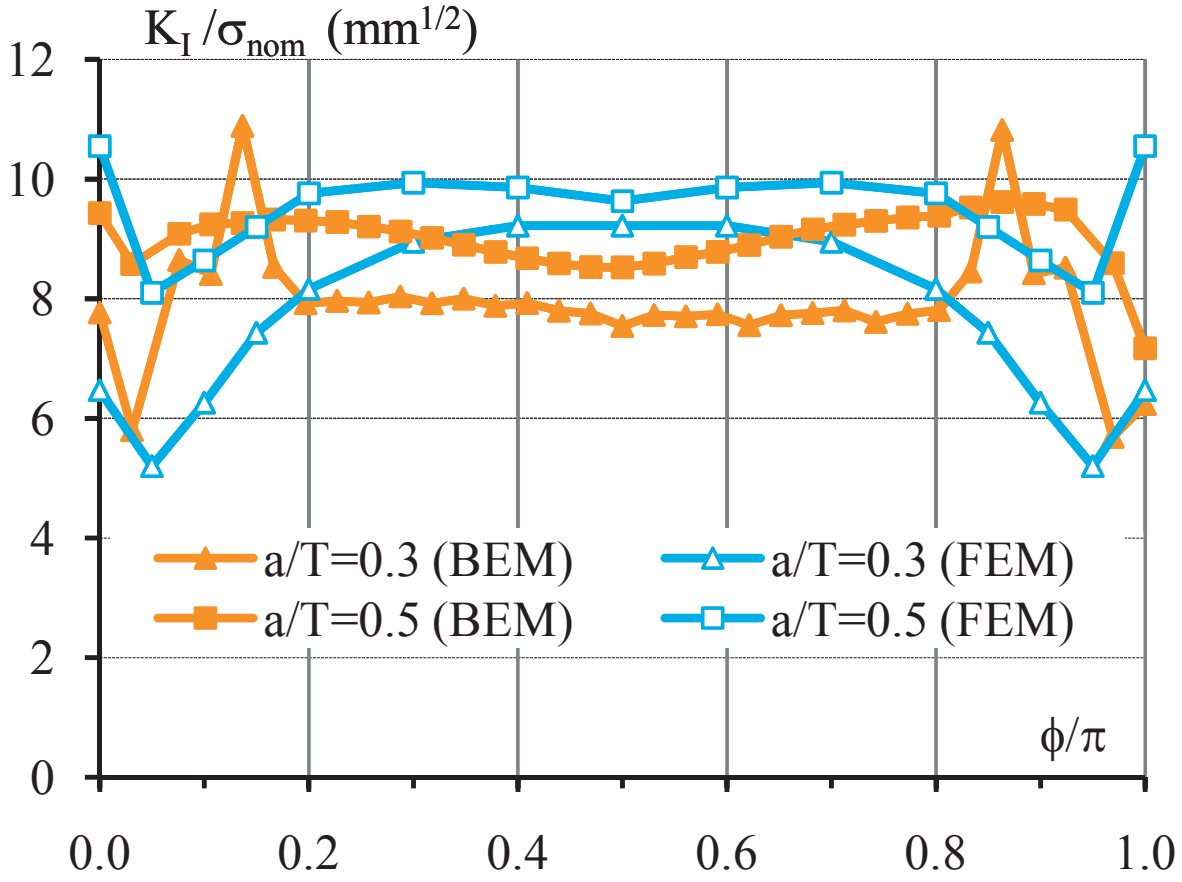

Accepted Manuscript
Not Copyedited

Copyright 2011 by the American Society of Civil Engineers

Fig 18

Journal of Bridge Engineering. Submitted October 25, 2010; accepted May 24, 2011;
posted ahead of print May 26, 2011. doi:10.1061/(ASCE)BE.1943-5592.0000274

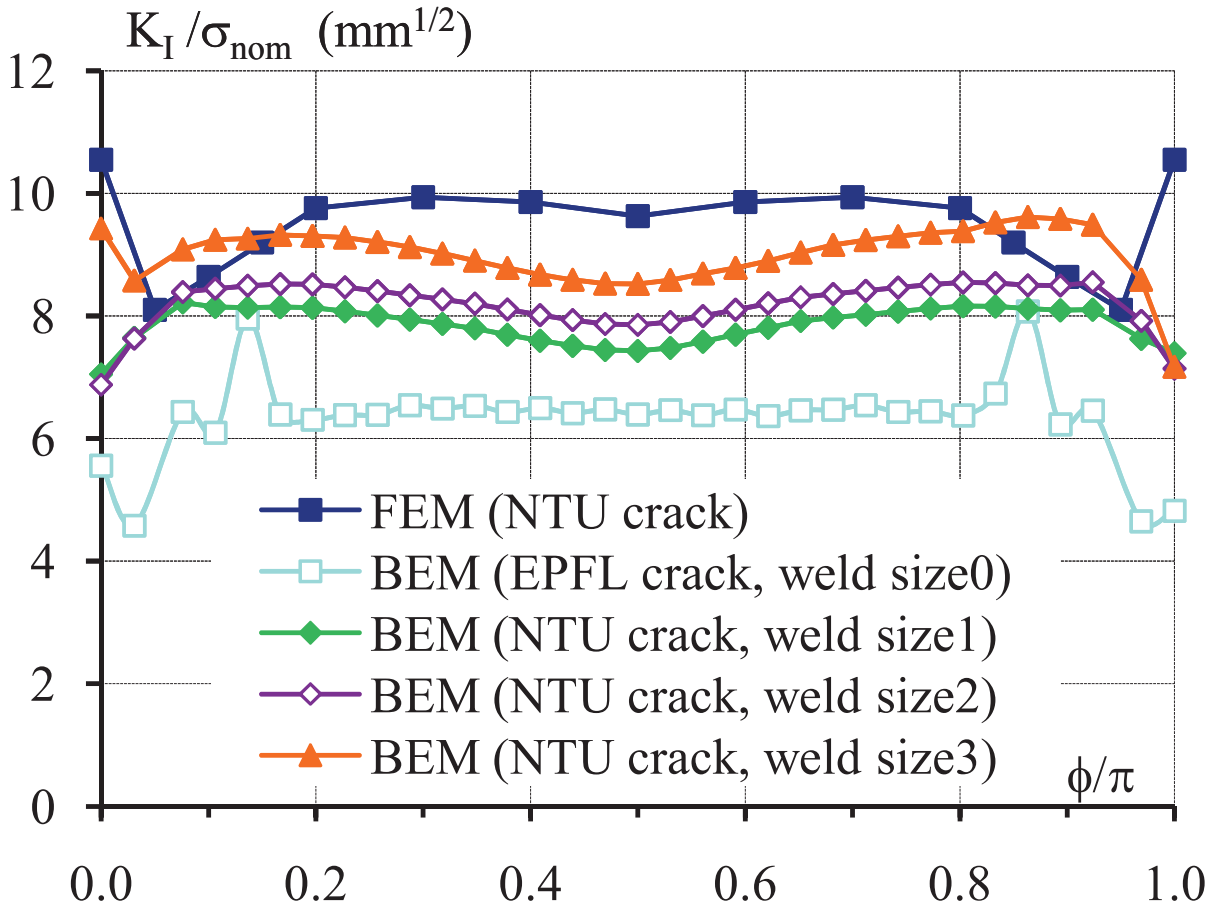

Accepted Manuscript
Not Copyedited

Copyright 2011 by the American Society of Civil Engineers

Fig 19

Journal of Bridge Engineering. Submitted October 25, 2010; accepted May 24, 2011;
posted ahead of print May 26, 2011. doi:10.1061/(ASCE)BE.1943-5592.0000274

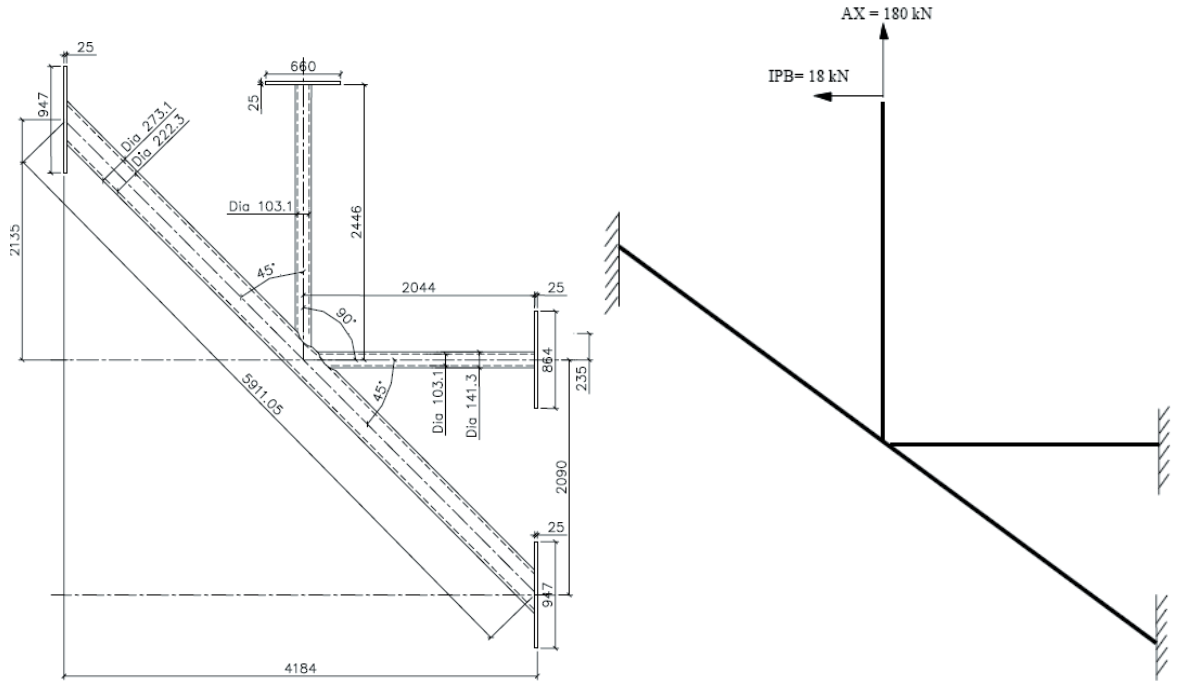

Accepted Manuscript
Not Copyedited

Copyright 2011 by the American Society of Civil Engineers

Fig 20

Journal of Bridge Engineering. Submitted October 25, 2010; accepted May 24, 2011;
posted ahead of print May 26, 2011. doi:10.1061/(ASCE)BE.1943-5592.0000274

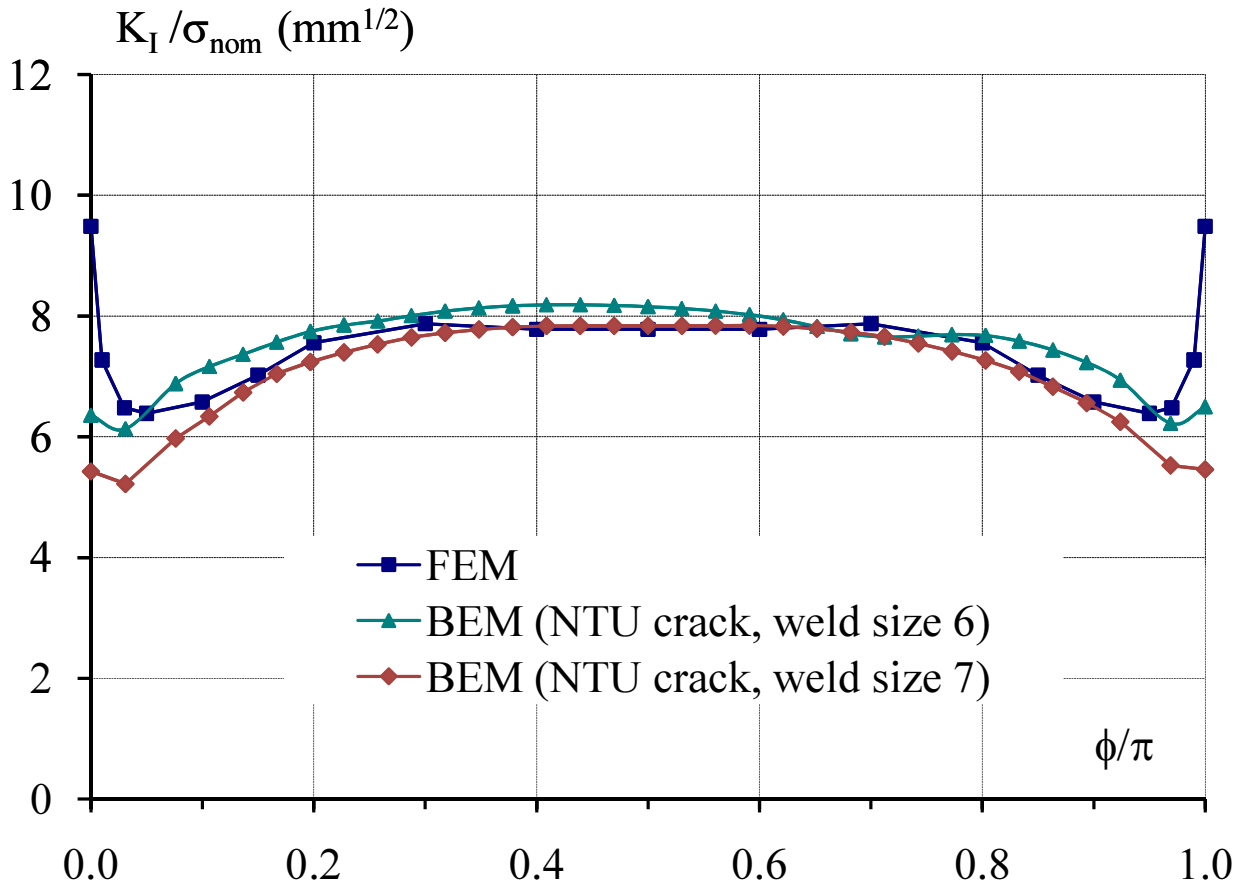

Accepted Manuscript
Not Copyedited

Copyright 2011 by the American Society of Civil Engineers

Fig 21

Journal of Bridge Engineering. Submitted October 25, 2010; accepted May 24, 2011;
posted ahead of print May 26, 2011. doi:10.1061/(ASCE)BE.1943-5592.0000274

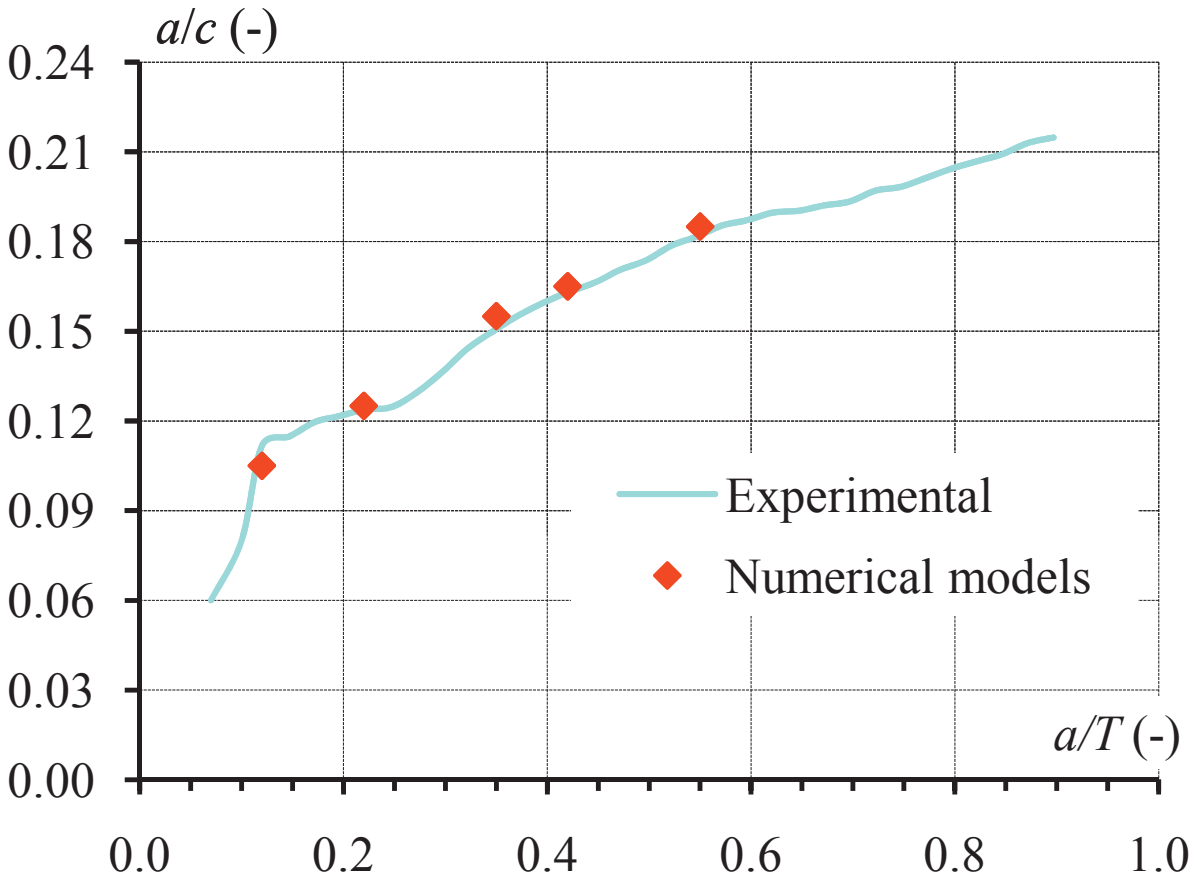

Accepted Manuscript
Not Copyedited

Copyright 2011 by the American Society of Civil Engineers

Fig 22

Journal of Bridge Engineering. Submitted October 25, 2010; accepted May 24, 2011;
posted ahead of print May 26, 2011. doi:10.1061/(ASCE)BE.1943-5592.0000274

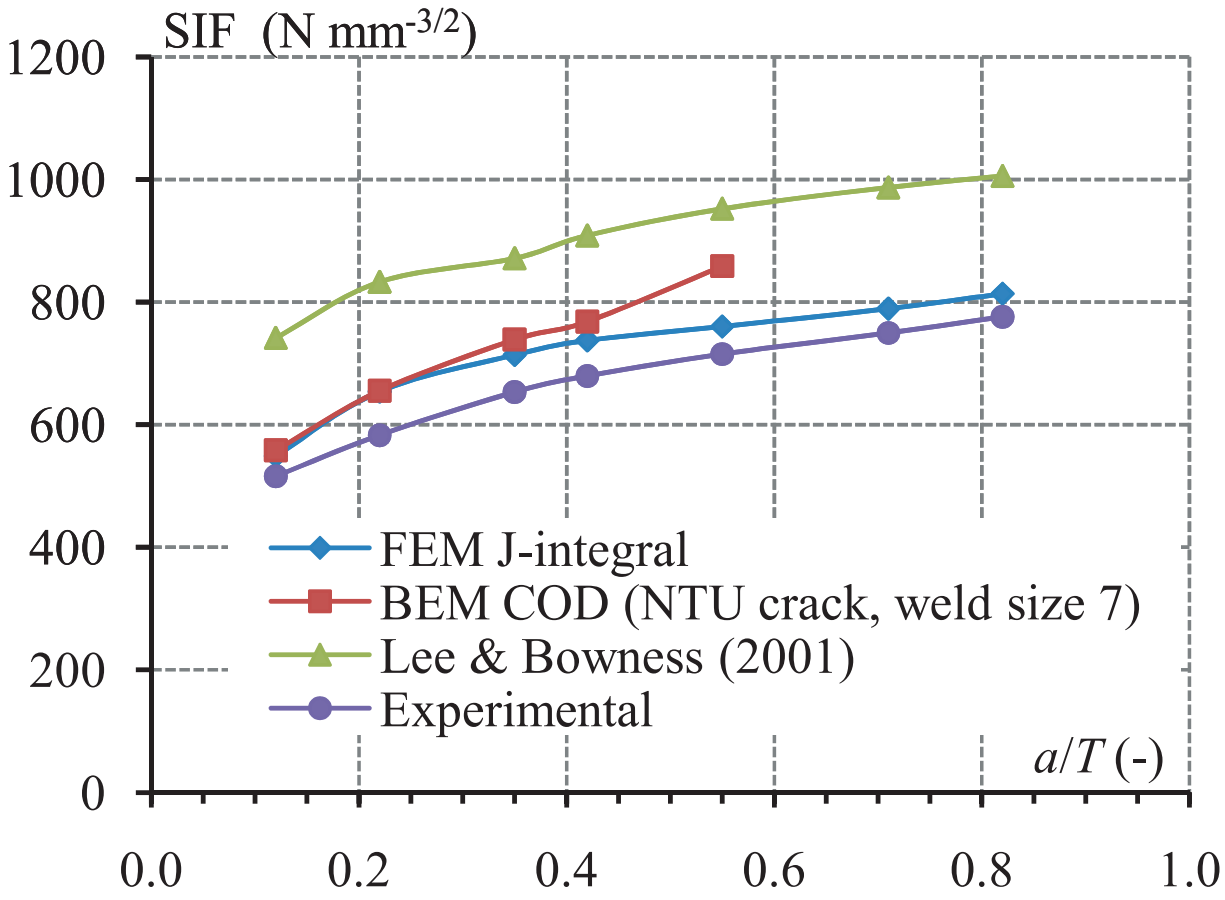

Accepted Manuscript
Not Copyedited

Copyright 2011 by the American Society of Civil Engineers